



MEaSURES ITS_LIVE Landsat Image-Pair Glacier and Ice Sheet Surface Velocities, Version 1

USER GUIDE

How to Cite These Data

As a condition of using these data, you must include a citation:

Gardner, A., M. Fahnestock, and T. Scambos. 2022 *MEaSURES ITS_LIVE Landsat Image-Pair Glacier and Ice Sheet Surface Velocities, Version 1* [Indicate subset used]. Boulder, Colorado USA. NASA National Snow and Ice Data Center Distributed Active Archive Center.

<https://doi.org/10.5067/IMR9D3PEI28U>

We also request that you acknowledge the author(s) of this data set by referencing the following peer-reviewed publication:

Gardner, A. S., G. Moholdt, T. Scambos, M. Fahnestock, S. Ligtenberg, M. van den Broeke, and J. Nilsson, 2018: Increased West Antarctic and unchanged East Antarctic ice discharge over the last 7 years. *The Cryosphere*, 12(2):521–547. <https://doi.org/10.5194/tc-12-521-2018>

FOR QUESTIONS ABOUT THESE DATA, CONTACT NSIDC@NSIDC.ORG

FOR CURRENT INFORMATION, VISIT <https://nsidc.org/data/NSIDC-0775>



National Snow and Ice Data Center

TABLE OF CONTENTS


1	DATA DESCRIPTION.....	2
1.1	Parameters	2
1.2	File Information	2
1.2.1	Format	2
1.2.2	File Contents	2
1.2.3	Naming Convention	3
1.3	Spatial Information	5
1.3.1	Coverage	5
1.3.2	Resolution.....	5
1.3.3	Geolocation	6
1.4	Temporal Information.....	6
1.4.1	Coverage	6
1.4.2	Resolution.....	6
2	DATA ACQUISITION AND PROCESSING	6
2.1	Acquisition.....	6
2.2	Processing	6
2.2.1	Image Preprocessing.....	6
2.2.2	Image Pair Velocities (autoRIFT v1).....	7
2.3	Quality, Errors, and Limitations	8
3	SOFTWARE AND TOOLS.....	9
4	VERSION HISTORY	9
5	RELATED DATA SETS	9
6	RELATED WEBSITES.....	9
7	CONTACTS AND ACKNOWLEDGMENTS.....	9
8	REFERENCES	10
9	DOCUMENT INFORMATION.....	11
9.1	Publication Date.....	11
9.2	Date Last Updated	11

1 DATA DESCRIPTION

The Inter-Mission Time Series of Land Ice Velocity and Elevation (ITS_LIVE) project, part of NASA's Making Earth System Data Records for Use in Research Environments (MEaSUREs) Program, was created to provide global, low-latency and, high temporal resolution measurements of glacier and ice sheet surface velocities and elevation changes.

This data set consists of velocities at 240 m resolution generated from satellite optical image pairs. Data are available for all land ice areas larger than 5 km² spanning the period from 1985 to 2018 (subject to image availability and quality). Velocities were derived by applying the autonomous Repeat Image Feature Tracking algorithm (autoRIFT) processing chain (Gardner et al., 2018; Lei et al., 2021) to imagery from Landsat 4, 5, 7, and 8. Data scarcity and/or low radiometric quality (e.g., band saturation) are significant limiting factors for many regions during the earlier years of the data record. Annual, global coverage is nearly complete after the 2013 launch of Landsat 8.

Note that Version 1.0 of this data set should be considered a beta version. A low-latency version is planned for future release.

 This data set is used to create the [MEaSUREs ITS_LIVE Regional Glacier and Ice Sheet Surface Velocities](#) product.

1.1 Parameters

Ice velocity (x and y components and velocity magnitude)

1.2 File Information

1.2.1 Format

The data are provided as NetCDF-4 (.nc) files.

1.2.2 File Contents

Each NetCDF file contains the variables listed in Table 1. Figure 1 is a plot of the velocity magnitude variable (v) for the Petermann Glacier in Greenland.

Table 1. Parameter Names and Descriptions

Parameter	Description	Units	Class
x	Map projected x coordinate	m	double
y	Map projected y coordinate	m	double
vx	Velocity component in x direction	m/yr	short
vy	Velocity component in y direction	m/yr	short
v	Velocity magnitude	m/yr	short
mapping	Projected Coordinate System (Polar Stereographic for images south of 70° S; UTM for non-Antarctic images)	-	float
interp_mask	Interpolated velocities mask (0 = measured, 1 = interpolated)	N/A	ubyte
img_pair_info	Information about image pair (e.g., satellite and sensor, acquisition and processing dates, processing level)	N/A	float
chip_size_width	Chip size width (in sample or x direction)	m	ushort
chip_size_height	Chip size height (in line or y direction)	m	ushort

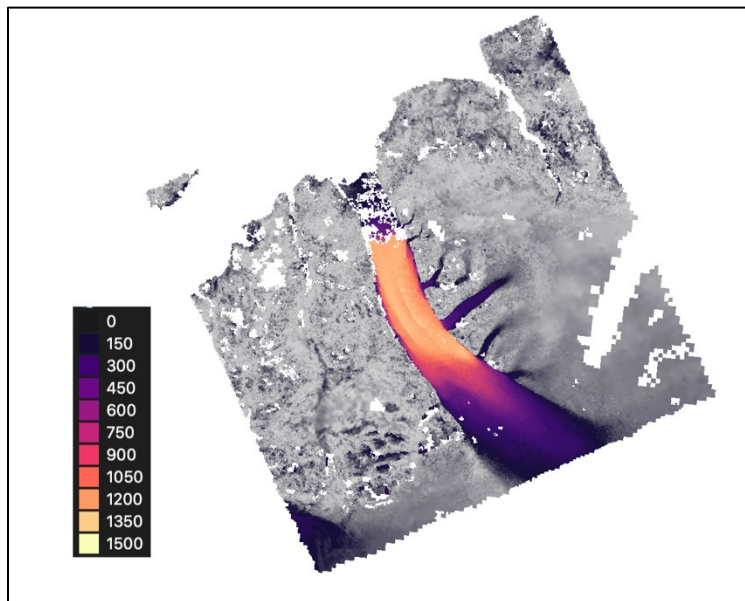


Figure 1. Velocity Magnitude (m/y), Petermann Glacier, Greenland

1.2.3 Naming Convention

Example File Name

LC08L1GT0600192013033001T2_LE07L1TP0600192011101201T1_32608_G0240V01_P002.nc

Naming Convention

- (1) [LXSS][LLLL][PPP][RRR][YYYYMMDD][CC]T[X]_
- (2) [LXSS][LLLL][PPP][RRR][YYYYMMDD][CC]T[X]_
- (3) [EEEE]_
- (4) G[RRRR]V[NN]_
- (5) P[HHH]

The naming convention, detailed in Table 2, consists of the five components, separated by underscore characters:

*{later image}_**{earlier image}_**{location code}_**{resolution, data set version}_**{pixel %}*
 (1) (2) (3) (4) (5)

The first two components contain information about the later (1) and earlier (2) images. They both utilize the following variables:

(1), (2) [LXSS][LLLL][PPP][RRR][YYYYMMDD][CC]T[X]

The third, fourth, and fifth components indicate:

- (3) Location (EEEE)
- (4) Spatial resolution (RRRR) and data version (NN)
- (5) Percentage of pixels with velocity estimates (HHH)

The following table describes the file name variables above:

Table 2. File Name Variables and Descriptions

Variable	Description
LXSS	L = Landsat X = Sensor ¹ : <ul style="list-style-type: none"> • C = OLI/TIRS Combined • O = OLI-only • T = TIRS-only • E = ETM+ • T = TM • M = MSS SS = Satellite number. E.g., Landsat 7 = 07.
LLLL	Landsat processing level ² : <ul style="list-style-type: none"> • L1TP = Precision Terrain • L1GT = Systematic Terrain • L1GS = Systematic
PPP RRR	PPP = WRS path RRR = WRS row

YYYYMMDD	Acquisition year (YYYY), month (MM), and day (DD)
CC	CC = Collection number. Collection 1 (01) or Collection 2 (02)
TX	TX = Collection category, preceded by "T": <ul style="list-style-type: none"> • T1 = Tier 1 (known tie points used to refine image geolocation) • T2 = Tier 2 (no tie points used, geolocation based on satellite ephemeris)
EEEE	Five-digit location code <ul style="list-style-type: none"> • Antarctic = 03031 • Northern non-Antarctic = 326xx (EPSG code, xx = local UTM Zone number) • Southern non-Antarctic = 327xx (EPSG code, xx = local UTM Zone number)
GRRRR	Spatial resolution of the velocity estimates, preceded by "G". E.g., G0240 = 240 m per pixel.
VNN	Data set version number, preceded by "V". E.g., V01 = Version 1.
PHHH	Percentage of total possible glacier pixels with reported velocities, preceded by "P". HHH indicates the percentage. E.g., P090 means that 90% of the possible glacier pixels have reported velocities.
.nc	NetCDF file extension

¹The ["What are the band designations for the Landsat satellites?"](#) webpage on the USGS website contains additional details about the different Landsat sensors.

²For more information, see [Landsat Levels of Processing](#)

1.3 Spatial Information

1.3.1 Coverage

Spatial coverage is global and includes all land areas with ice bodies larger than 5 km² (depending on data availability, quality, and offset tracking success).

The spatial extent of any given image pair depends on the offset tracking success for that pair, and thus two granules encompassing image pairs with the same Landsat path and row designations can have different extents. For example, if one of the input images was largely cloud covered, the coverage in the output area can be significantly reduced from the original image extent.

1.3.2 Resolution

ITS_LIVE image pair granules comprise one ice flow vector per 240 m x 240 m area tracked by autoRIFT.

1.3.3 Geolocation

Each image pair granule in this release uses the original USGS selected projection of the Landsat input images (with the exception of some images that were reprojected near UTM zone boundaries). For non-Antarctic images, this projection is the local UTM—EPSG:326xx (northern) and EPSG:327xx (southern)—where xx is the UTM zone number. Images south of 70° S utilize the SCAR Antarctic Polar Stereographic projection (EPSG:3031).

1.4 Temporal Information

1.4.1 Coverage

1985 to 2018

1.4.2 Resolution

The separation time between image pairs varies from 6 to 546 days.

2 DATA ACQUISITION AND PROCESSING

2.1 Acquisition

The data set utilizes imagery from the following sources:

- Landsat 4 Thematic Mapper, Band 2 (1982 to 1993)
- Landsat 5 Thematic Mapper, Band 2 (1984 to 2013)
- Landsat 7 Enhanced Thematic Mapper Plus, Band 8 (1999 to 2018)
- Landsat 8 Operational Land Imager, Band 8 (2013 to 2018)

All images with $\leq 60\%$ cloud cover (per the image metadata) were processed. Landsat imagery was provided courtesy of the USGS and downloaded from Google Cloud (<https://cloud.google.com/storage/docs/public-datasets/landsat>).

2.2 Processing

2.2.1 Image Preprocessing

All images were preprocessed using a 5×5 Wallis operator to normalize for local variability in image radiance due to shadows, topography, and sun angle, which can produce artifacts in surface flow derived from feature tracking. For Landsat 4 and 5, Fourier filtering was used to remove along-track artifacts introduced by the Thematic Mapper whisk broom sensor. Missing Landsat 7 images,

due to the Scan Line Corrector failure (SLC-off) in May of 2003, were filled with random noise to prevent them from contributing to the correlation peak amplitude used by the feature tracking.

2.2.2 Image Pair Velocities (autoRIFT v1)

This data set is generated by using Version 1 of autoRIFT (Gardner et al., 2018) to identify surface displacements in image pairs from repeat orbits and adjacent or near-adjacent orbits lying within a specified distance. Furthermore, image pairs were only collected from the same satellite position (“same-path-row”) when separated in time by fewer than 546 days. This approach was used for all satellites in the Landsat series (L4 to L8).

To increase data density prior to the launch of Landsat 8, images acquired from differing satellite positions—generally in adjacent or near-adjacent orbit swaths (i.e., “cross-path-row”)—are also processed if they have a time separation between 10 and 96 days and an acquisition date prior to when operational Landsat 8 data began on 14 June 2013.

Feature tracking of cross-path-row image pairs produces velocity fields with a lower signal-to-noise ratio due to residual parallax from imperfect terrain correction. Matching features in pre-processed, same-path-row and cross-path-row image pairs were identified by using a Gaussian kernel to oversample the correlation surface by a factor of 16 and find local, normalized cross-correlation (NCC) maxima at sub-pixel resolutions.

A sparse grid, pixel-integer NCC search (1/16 of the density of full search grid) was used to determine areas of coherent correlation between image pairs (see the Normalized Displacement Coherence filter described in Gardner et al., 2018). Results from the sparse search were then used to guide a dense search, which spaces search centers such that no overlap exists between adjacent template windows. Areas of unsuccessful retrievals, as determined by the NDC filter, were searched with progressively increasing template chip sizes. Minimum and maximum acceptable template chip sizes for each search center were defined geographically depending on land surface type (ice or rock); spatial gradient of a reference velocity mapping; distance from the ocean; and distance from an ice edge. The data were then filtered one last time using the NDC filter, followed by a light interpolation to fill in small data gaps. The location of interpolated values are recorded in `interp_mask` with a value of “1”.

To reduce computational demand, autoRIFT employs a downstream search that centers the NCC search template window in the search image at the downstream location of the expected displacement between the two image pairs, as determined from the reference velocity. The NCC search radius is unique in both the x and y directions and varies spatially. It is defined according to the surface type (ice or rock), magnitude of the component reference velocity (v_x , v_y), and the

distance from the ocean. Ocean area is identified according to the [Global Self-consistent, Hierarchical, High-resolution Geography Database \(GSHHG\)](#).

Land ice in Greenland was identified using a data set provided by F. Paul (Bolch et al., 2013); Antarctica land ice was identified using Depoorter et al. (2013). Everywhere else, land ice is determined using the Randolph Glacier Index release 3.2 (see <https://www.glims.org/RGI/>). Rock is defined as neither ocean nor land ice.

For more information, see the [ITS_LIVE Regional Glacier and Ice Sheet Surface Velocities product](#).

2.3 Quality, Errors, and Limitations

Image geometry between same-path-row image pairs is highly stable; however, geolocation errors of up to 15 m can exist in the x and y coordinate. If uncorrected, a geolocation error of, say, $\sqrt{15^2 + 15^2} = 21$ m between two images separated in time by 16 days would introduce a bias in velocity of as much as 480 m/yr. To correct for these errors, the component velocities v_x and v_y are tied to a “stable” surface—the median of each velocity component is set to zero over rock surfaces and set to the median reference velocity over slow-moving areas (ice movement of <15 m/yr) of Greenland and Antarctica. For Greenland, the [MEaSURES Greenland Annual Ice Sheet Velocity Mosaics from SAR and Landsat, Version 1](#) data are used as the reference velocity; for Antarctica, the [MEaSURES InSAR-Based Antarctica Ice Velocity Map, Version 2](#) data are used.

The uncertainty for each image pair velocity field is set equal to the standard deviation in component velocities measured over a stable surface after applying the geolocation offset correction (if available). If an image pair velocity field does not intersect a stable surface, the errors in v_x and v_y are set to the root sum of the squares (RSS) of the pointing uncertainty of both images. If the image pair velocity is successfully co-registered during the creation of the annual mosaic (see below), this error is updated to the standard deviation of the difference between the image pair component velocities and the annual mean component velocities.

Velocities are calculated from imagery that has been map projected. This can introduce scale errors of up to a few percent that are dependent on the projection used and the location of the imagery. This distortion is corrected for such that derived velocities represent horizontal velocities that would be measured by an observer on the ground. This has several implications:

1. When using ITS_LIVE image pair velocities to calculate glacier flux, the flux-gate cross-section needs to be corrected for projection scale distortion (the image pair velocities do not need to be corrected).

2. When calculating Lagrangian paths in map coordinates, image pair velocities should be scaled from velocities in ground units to velocities in map units, to produce the appropriate speed in map coordinates.

3 SOFTWARE AND TOOLS

NetCDF files can be opened using a wide range of software. For further details, see [Software for Manipulating or Displaying NetCDF Data](#). The metadata fields can be extracted using the gdalinfo command line utility available from the [Geospatial Data Abstraction Library \(GDAL\)](#) website.

4 VERSION HISTORY

Version 1 (September 2022)

5 RELATED DATA SETS

Note: The data sets listed below are examples of the many already published products related to the ITS_LIVE project.

- [MEaSURES ITS_LIVE Regional Glacier and Ice Sheet Surface Velocities](#)
- [Global Land Ice Velocity Extraction from Landsat 8 \(GoLIVE\)](#)
- [Landsat 8 Ice Speed of Antarctica \(LISA\)](#)
- [MEaSURES Greenland Ice Velocity: Selected Glacier Site Velocity Maps from InSAR](#)
- [MEaSURES Annual Antarctic Ice Velocity Maps 2005-2017](#)

6 RELATED WEBSITES

- [MEaSURES data at NSIDC | Overview](#)

7 CONTACTS AND ACKNOWLEDGMENTS

Alex Gardner

Sea Level and Ice Group

Jet Propulsion Laboratory

California Institute of Technology

La Cañada Flintridge, CA

Mark Fahnestock

Geophysical Institute
University of Alaska Fairbanks
Fairbanks, AK

Ted Scambos

Earth Science & Observation Center
University of Colorado Boulder
Boulder, CO

8 REFERENCES

Bolch, T., Sandberg Sørensen, L., Simonsen, S. B., Mölg, N., Machguth, H., Rastner, P., & Paul, F. (2013). Mass loss of Greenland's glaciers and ice caps 2003-2008 revealed from ICESat laser altimetry data. *Geophysical Research Letters*, 40(5), 875–881. <https://doi.org/10.1002/grl.50270>

Depoorter, M. A., Bamber, J. L., Griggs, J. A., Lenaerts, J. T. M., Ligtenberg, S. R. M., van den Broeke, M. R., & Moholdt, G. (2013). Calving fluxes and basal melt rates of Antarctic ice shelves. *Nature*, 502(7469), 89–92. <https://doi.org/10.1038/nature12567>

Gardner, A. S., Moholdt, G., Scambos, T., Fahnestock, M., Ligtenberg, S., van den Broeke, M., & Nilsson, J. (2018). Increased West Antarctic and unchanged East Antarctic ice discharge over the last 7 years. *The Cryosphere*, 12(2), 521–547. <https://doi.org/10.5194/tc-12-521-2018>

Joughin, I., Smith, B. E., Howat, I. M., Scambos, T., & Moon, T. (2010). Greenland flow variability from ice-sheet-wide velocity mapping. *Journal of Glaciology*, 56(197), 415–430. <https://doi.org/10.3189/002214310792447734>

Lei, Y., Gardner, A., & Agram, P. (2021). Autonomous Repeat Image Feature Tracking (autoRIFT) and Its Application for Tracking Ice Displacement. In *Remote Sensing* (Vol. 13, Issue 4). <https://doi.org/10.3390/rs13040749>

Mouginot, J., Scheuchl, B., & Rignot, E. (2012). Mapping of Ice Motion in Antarctica Using Synthetic-Aperture Radar Data. *Remote Sensing*, 4(9), 2753– 2767. <https://doi.org/10.3390/rs4092753>

Rignot, E., Mouginot, J., & Scheuchl, B. (2011). Ice Flow of the Antarctic Ice Sheet. *Science*, 333(6048), 1427–1430. <https://doi.org/10.1126/science.1208336>

9 DOCUMENT INFORMATION

9.1 Publication Date

September 2022

9.2 Date Last Updated

September 2022